

# Comparison of Used Locomotive Fuel Filters after Using B20 and B0 Fuels

ihwan haryono

BPPT: Badan Pengkajian dan Penerapan Teknologi <https://orcid.org/0000-0003-1426-9097>

Muhammad Ma'ruf (✉ [muhammad.maruf@bppt.go.id](mailto:muhammad.maruf@bppt.go.id))

BPPT: Badan Pengkajian dan Penerapan Teknologi <https://orcid.org/0000-0002-5460-9810>

Hari Setiapraja

BPPT: Badan Pengkajian dan Penerapan Teknologi

Dieni Mansur

LIPI: Lembaga Ilmu Pengetahuan Indonesia <https://orcid.org/0000-0002-0535-7768>

---

## Research

**Keywords:** Palm biodiesel, fatty acid methyl ester, used fuel filter, locomotive, periodic maintenance

**Posted Date:** June 16th, 2021

**DOI:** <https://doi.org/10.21203/rs.3.rs-516328/v1>

**License:** © ⓘ This work is licensed under a Creative Commons Attribution 4.0 International License.

[Read Full License](#)

---

# Abstract

The automotive and non-automotive sectors have followed the Indonesian government's policy regarding applying high concentration biodiesel use. Some issues arise from the effects of using a high biodiesel concentration on engine components, such as filter blocking or degradation. Therefore, various parties have challenged to improve both in terms of fuel quality and engine components. Meanwhile, testing of high concentration biodiesel fuel (blending ratio above 10 %) was still rarely published in the rail transport sector. Therefore, the rail test aimed to evaluate the effect of B20 fuel on locomotive engine components. The test was conducted during two periodic maintenance (6 months) using two trains with B20 and B0 fuels as a comparison. This study discusses the effect of B20 on fuel filters by performing tests on used filters for one periodic maintenance (3 months). The morphological analysis of deposits was conducted using a digital microscope, while TGA, GC-MS, FTIR, and elemental analysis were used to determine its components. The results showed that biodiesel filtration in the main filter was higher, and the subsequent filtration showed fewer deposits than that of pure diesel. Various types of fuel filter deposits have been identified, such as hydrocarbons and fatty acid methyl esters.

## 1. Introduction

The Indonesian government's policy on applying high concentration biodiesel has been followed by developing engine technology in the automotive sector, such as improving engine components, handling, and storage systems. Studies on the effects of using biodiesel fuel are easy to obtain from various publications. Nevertheless, biodiesel's use and test in the rail transport sector were lagging, especially for locomotive with high ratio fuel and a blending volume above 10 %. It was reported that using high biodiesel concentration causes problems in the intake system and engine components [1], such as filter clogging. Several case studies have reported that biodiesel was beneficial in minimizing exhaust emissions (except NO<sub>x</sub>) without significantly reducing engine performance but at risk of clogging the filter and reducing fuel economy [2].

The use of biodiesel with high concentrations affects deposit formation that caused accelerating the replacement time of the vehicle filter [3–6]. Apart from the contaminant factor, the excess deposit formation is also caused by ester compounds in the fuel. Testing of deposit characteristics was carried out by Csontos et al. with analysis using GC-MS, XRF-EDX, FTIR, and TGA. They identified carboxylic acid (CA) as fuel degradation and unreacted CA from biodiesel production, oxidized polymer compounds, glycerol, sterol, other impurities, and contaminants [7, 8]. Meanwhile, Barker et al. identified the deposit or injector fouling as carbon in nature with C<sub>16</sub>-C<sub>18</sub> acid/ester [9]. However, several publications reported no significant difference in filters with pure diesel oil from petroleum [10, 11]. Lammert et al. stated that low environmental temperatures such as during winter, the replacement of fuel with biodiesels disrupted the cold flow properties [12].

Our previous studies related to locomotive engines have identified that filter deposits are in the form of materials from fuel degradation, impurities from unreacted biodiesel production, as well as wear and

contaminants. The results showed that the use of 20 % of palm oil during one maintenance period still guarantees a good filtration performance [13]. The effect of 20 % biodiesel (B20) fuel with strict quality control to the locomotive engine after being used for one maintenance period (3 months) from the rail test for 6 months, the used filters were investigated. This study reported the test results that compared them with petrodiesel fuel (B0).

## 2. Materials And Methods

### 2.1 Materials

B20 (20 % biodiesel and 80 % petrodiesel by volume) and B0 (100 % petrodiesel by volume) fuels were used for the locomotive engine. The biodiesel was derived from palm oil, which met the national quality standard (SNI 7182:2015), contained 0.8 % mass of Monoglyceride (MG), and less than 500 ppm moisture content. Furthermore, the petrodiesel met the national standard Decree of the Director-General of Oil and Gas Number 28.K/10/DJM.T/ 2016 and contained less than 2500 ppm sulfur with 48 cetane number.

### 2.2 Testing Methods and Analysis

The filter test was carried out on a coal-carrying train locomotive engine. One train uses B20 fuel, and the other uses B0 for comparison. Furthermore, the trains were run daily for 3 months, which is equivalent to 1 periodic maintenance. After 3 months, the filter was removed and replaced with a new one.

Subsequently, the filter was virtually analyzed with a 3D digital microscope (KH-8700, Hirox Co., Ltd.). Trapped materials or chemicals were analyzed by a gas chromatography-mass spectrometry (GC-MS), Fourier-transform infrared spectroscopy (FTIR), an elemental analyzer, thermogravimetric analysis (TGA), and differential thermogravimetric (DTG). Before GC-MS analysis, the filter was cut around 1 cm<sup>2</sup> and then soaked in 10 mL of each acetone, chloroform, dichloromethane (DCM), and n-hexane as organic solvents. Meanwhile, solvents containing precipitate matter were filtered using a filter paper (Whatman, Glass microfiber filters GF/F diameter 47 mm, pore diameter 0.7 μm, Cat No. 1825-047) to prevent tiny solid particles from entering the GC-MS column. The use of these solvents was intended to determine the most effective in dissolving precipitate.

The GCMS model, 6890 N (Agilent Technologies Inc., Santa Clara, California, United States), was equipped with a mass spectrometer detector, 5975B and HP-5MS UI column (Agilent Technologies, 5 % Phenyl Methyl Siloxane, 30 m × 250 μm × 0.25 μm). Furthermore, the injector temperature was 250°C, and the carrier gas was helium at a constant flow rate of 1 mL min<sup>-1</sup>. The initial oven temperature of the column was 40°C, which was maintained for 1 min, raised to 300°C at 10°C min<sup>-1</sup>, and then maintained for 4 minutes at 300°C. The MS Source and MS Quad temperatures were 230°C and 150°C, respectively. Also, ionization energy was 70 eV, and the total flow was 104 mL min<sup>-1</sup>, column flow was 1 mL min<sup>-1</sup>, and the average velocity was 36.262 cm s<sup>-1</sup>. Chemicals identification in the samples was determined by

comparing spectra and retention time of the individual compounds with the authentic references stored in the NIST14 mass spectral data library.

The FTIR (IR Prestige 21, Shimadzu instrument) technique was used in the wavenumber range of 4000–400  $\text{cm}^{-1}$  to identify functional groups of chemical contents in the filter engine containing precipitate. Meanwhile, the used filter using B20 fuel was analyzed by thermogravimetric analysis (TGA) to ascertain its thermal characteristics. Also, a new filter was analyzed as a comparison. TGA is a technique to monitor changes in the mass of a material to temperature and time [14]. The small size of the used and a new filter as comparison were put into a thermogravimetric analyzer (STA PT 1600, Linseis), and then the sample was heated in  $\text{N}_2$  atmosphere from room temperature (about 30°C) to 600°C at a rate of 10°C/min to obtain the weight loss profile. Moreover, an elemental analyzer (CHN 628 series, Leco Corporation), according to the ASTM D 5373 procedure, was used to analyze elemental content in the used and new filters as a comparison.

## 2.3 Locomotive Engine for Testing

The locomotive engine specifications used in this test are shown in Table 1. This engine has three levels of fuel filtration. The first level was a strainer for filtering contaminants with sizes above 10 microns and water. The second level was the main filter for particles with a size of 5–10 microns, while the third one was the twin filter to filtrate smaller particles that stick to the engine. The schematic of the test engine filtration system is shown in Fig. 1. The main and twin filters were virtually analyzed using a 3D digital microscope, while the main filter was analyzed using GCMS, TGA, FTIR, and elemental analyzer.

Table 1  
Specifications of the test locomotive engine

Main component	Specification
Manufacturing company	Electro Motive Diesel (EMD)
Model	GT 38 AC
Diesel motor	8-710 G3BES-T2
Type	2 stokes 8 cylinders with after cooler turbocharger
Fuel injection	Electronic controlled
Recommended fuel	HSD
Transmission	Electric, AC/AC
Gross HP	2200
Maximum speed (km/jam)	90

## 3. Results And Discussion

This study determines using B20 on the main and twin filters after 3 months of use. Furthermore, filter analysis with B0 fuel was conducted on these two types of filters as references, and strainers for B20 and B0 were not analyzed because they only captured large-size material (such as rocks or gravel). Therefore, deposits of B20 fuel were not captured.

### *3.1 Photo of Fuel Filter*

The visual inspection result of the used main filters with B20 and B0 fuel after 3 months using a 3D digital microscope at a magnification of 500 times is shown in Figure 2. While the deposit's thickness was assessed at 100 times magnification, as shown in Figure 3.

In the used main filter for B20, it can be seen that the fibers have been tightly covered with a material deposit, while for the B0, the fiber and porosity were still clearly visible. The result of deposit thickness measurement showed that B20 was higher with an average of 822  $\mu\text{m}$  compared to B0 with an average of 699  $\mu\text{m}$ . Meanwhile, the type of deposit on the main filter with B20 fuel was soft, and hence, even though it appeared to cover the surface, fuel still flowed with less resistance, and the delta pressure filter test did not change significantly. Likewise, the performance test results showed that the decrease of power was not significant after using B20 for 3 months [15].

Figures 4 and 5 show the deposit's morphology on the twin filter for B20 and B0 with a 200 and 500 times magnification, respectively. It can be seen that after 3 months of usage, the fibers were still visible, both for the used filters of B0 and B20. However, the granule deposit which covers the filter surface had a different size. Petrodiesel (B0) tent formed a smaller size of granule deposit compared with B20.

The cross-section of the deposit thickness show that B20 has an average of 601  $\mu\text{m}$  and B0 has 621  $\mu\text{m}$  as shown in Figure 6. This can be considered because the contaminants for B20 have been filtered on the main filter, hence, the filtration process at twin filter is lighter.

### *3.2 Identification of trapped materials or chemicals on the filter*

Analysis with GCMS was conducted to determine which deposit components were filtered on the main and twin filters with B20 or B0 fuels. Furthermore, the identification of trapped materials or chemicals on the used filter was analyzed by FTIR, elemental analyzer, and TGA. The used filters were soaked in four organic solvents before GC-MS analysis, namely acetone, chloroform, dichloromethane (DCM), and n-hexane. The identified chemicals on this filter using B0 fuel for each solvent are shown in Table 2.

According to Table 2, among the four organic solvents used to dissolve chemicals in the used filter, chloroform appears to be better than acetone, dichloromethane, and n-hexane due to many chemicals identified. There were two compounds not identified with the chloroform solvent but identified with the n-hexane solvent. The results of the identified compounds were a combination of compounds dissolved in chloroform and n-hexane. Therefore, the chemical compounds contained in the filters were obtained. Based on the combination identified compounds with chloroform and n-hexane (Table 2), the chemicals

trapped on the used filter were hydrocarbons with the number of atoms of  $C_{12} - C_{27}$ , and the dominant one was pentadecane, 2,6,10,14-tetramethyl- ( $C_{19}H_{40}$ ). Alkane hydrocarbon compounds over  $C_{16}$  are solid at 20 °C. Therefore,  $C_{17}$  and above were naturally trapped and caused a blockage on the filter.  $C_{12} - C_{16}$  compounds were identified because there was no pretreatment to the filter before soaking in the organic solvent, meaning that it was still left on the filter, although the hydrocarbons  $C_{12} - C_{16}$  at 20 °C in the liquid phase.

Furthermore, naphthalene compounds caused blockage because of a high melting point and solid at room temperature. As the main diesel component, the alkane group dominated the precursor deposits. The deposit contained tetradecane, pentadecane, and hexadecane.

The identified chemicals on the used filter with B20 fuels for each solvent can be seen in Table 3. Based on Table 3, chloroform was a better solvent than others in dissolving chemicals trapped on the used filter with B20 fuel. However, some compounds could not be dissolved by chloroform but dissolve in acetone, DCM, and n-hexane. The chemicals identified in the four organic solvents were combined as shown in Table 3, with the percentage of peak areas mainly dissolved in chloroform. The chemicals were alkane hydrocarbons and fatty acid methyl ester, mainly Hexadecanoic acid, methyl ester ( $C_{15}H_{30}O_2$ ), and 9-Octadecenoic acid, methyl ester, (E) - ( $C_{19}H_{36}O_2$ ).

The hydrocarbons were almost the same as Table 2, which was derived from petrodiesel. Meanwhile, fatty acid methyl ester compounds derived from palm biodiesel. Chemical compounds such as Methyl tetradecanoate and Tridecanoic acid 12-methyl-, methyl ester were derived from Fatty acid  $C_{14}$  (myristic acid) that solid phase at room temperature. Likewise, Hexadecanoic acid, methyl ester, and Methyl stearate derived from  $C_{16:0}$  (palmitic acid) and  $C_{18:0}$  (stearic acid) fatty acids, respectively, can cause filter blockage. Next, 8,11-Octadecadienoic acid, methyl ester, and 9-Octadecenoic acid, methyl ester, (E)- were derived from  $C_{18:1}$  fatty acid (oleic acid) that liquid phase at room temperature. Therefore, it can be concluded that the large peak areas (corresponded to high concentrations) of Hexadecanoic acid, methyl ester ( $C_{15}H_{30}O_2$ ) and 9-Octadecenoic acid, methyl ester, (E) - ( $C_{19}H_{36}O_2$ ) were caused by a high concentration of palmitic and oleic acid in the palm oil and no pretreatment on the used filter before soaking. Nevertheless, methyl esters derived from oleic acid do not cause filter blocking. Therefore, the precursor deposit component for the B20 filter was dominated by fatty acid methyl esters, although based on the measurement results, the deposit was also caused by alkane hydrocarbons.

Moreover, the used filter with B20 fuel was analyzed by FTIR to support chemical identification of the GC-MS results and compared with the new one. The FTIR analysis results and prediction of functional groups for each peak are shown in Figure 7 and Table 6, respectively.

Based on FTIR analysis, the peaks that appeared on a new filter generally also appeared on the used filter. However, several new peaks appeared on the used filter, such as wave numbers 1259 and 1232  $cm^{-1}$  which were predicted to be the C-O-C group from ester, which was probably derived from biodiesel.

Furthermore, the predicted wavenumbers 626 and 468  $\text{cm}^{-1}$  were the naphthalene groups. The peak at wave number 609  $\text{cm}^{-1}$  was predicted as -SO<sub>2</sub>- group derived from petrodiesel fuel.

The used filter is also analyzed with an elemental analyzer to determine the percentage of carbon, hydrogen, and oxygen in the filter compared to the new one, as seen in Table 7. Elemental analysis results showed that the contents of carbon [C] and hydrogen [H] in the used filter increased compared to the new one by 20.4 % and 3 %, respectively, caused by fuel or engine crust passed through the filter. The nitrogen [N] content was very small and can be neglected as a trace element. Meanwhile, the oxygen content [O] in the new filter was the oxygen from the filter material. The oxygen content in the used filter was lesser than the new one because of high added carbon from trapped fuel, while the O value was calculated based on the difference between the percentages of C, H, and N. As the percentage of C and H increased, the O percentage decreased. The value of detected O in the used filter was predicted derived from the filter component, fuel, or sulfur. Also, sulfur estimation was known from FTIR analysis at peak 609  $\text{cm}^{-1}$  (Table 6) because the elemental analyzer could only detect C, H, and N.

Moreover, the used filter was analyzed by Thermogravimetric (TG) and Differential Thermogravimetric (DTG) analysis to understand its thermal properties compared with the new filter. Figure 8 shows the TG and DTG analysis results of the used and the new filters at N<sub>2</sub> conditions with a heating rate of 10  $^{\circ}\text{C min}^{-1}$  from room temperature to 600  $^{\circ}\text{C}$ . Comparing the TG and DTG curves between the used (Figure 8a), and the new filters (Figure 8b) showed thermal degradation of the used filter consisted of three decomposition areas, namely 35 - 150  $^{\circ}\text{C}$ ; 150 - 320  $^{\circ}\text{C}$ ; and 320 - 400  $^{\circ}\text{C}$ , while the new one only consisted of two areas of 35 - 150  $^{\circ}\text{C}$  and 250 - 400  $^{\circ}\text{C}$ . In 35 - 150  $^{\circ}\text{C}$ , it was predicted as water evaporation and volatile compounds decomposed from the filter material. Furthermore, in the new filter, the next decomposition occurred at 250 - 400  $^{\circ}\text{C}$ , which was predicted the larger molecular weight material, such as polymer or composite, be decomposed. Next, in the used filter at 150 - 320  $^{\circ}\text{C}$  decomposition or evaporation of fuel with the number of carbon atoms [C] ranging from C<sub>13</sub> - C<sub>18</sub> such as Tridecane, Tetradecane, Pentadecane, Hexadecane, Tridecane, and Octadecane (Table 2 and 3). Meanwhile, in 320 - 400  $^{\circ}\text{C}$ , there was decomposition or evaporation of a larger number of carbon atoms [C] ranging from C<sub>19</sub> - C<sub>27</sub>, such as Nonadecane, Eicosane, Heneicosane, Docosane, Tricosane, Heptacosane, Tetracosane, Pentacosane, and Eicosane.

## 4. Conclusion

The amount of trapped deposit material on the B20 filter showed that the first (main filter) was more than B0, and the material passed to the second filter (twin filter) was less. During one periodic maintenance, the main pores of the B20 filter have been closed by substrate, while on the twin filters, the use of B20 and B0 fuels still showed the porosity. Moreover, the used filter of rail locomotive fueled by B20 was identified various deposit compounds which contained hydrocarbon chains of C<sub>13</sub> - C<sub>27</sub> and fatty acid methyl esters C<sub>15</sub> - C<sub>19</sub>. Furthermore, deposit formation on both B0 and B20 was at tolerance level so that it did not require faster changing.

# Declarations

## Acknowledgements

The authors deeply acknowledge sincere gratitude towards BPDPKS, EBTKE, PT. KAI, PT. PERTAMINA, PT APROBI and all team members who supported the studies.

## Authors' contributions

All the authors contributed equally to this article. MM & DM tested the samples and interpreted data. IH collected the data, other information, and drafted the article. HS conducted major reviews, edits, and add the analysis.

## Funding

This study was funded by BPDPKS and supported by EBTKE, PT. KAI, PT. PERTAMINA, PT APROBI.

## Availability of data and materials

All data generated or analyzed during this study are recorded from Experimentation.

## Competing interests

The authors declare no conflict of interest. The funders had no role in the study design in collecting, analyzing, or interpreting data or the article's writing.

# References

1. Charlotte Stead, ZiaWadud, Chris Nash and Hu Li. Introduction of Biodiesel to Rail Transport: Lessons from the Road Sector. 2019. Sustainability MDPI.
2. Ian Skinner et.al. Railways and Biofuel. 2007. First UIC Report.  
[https://uic.org/IMG/pdf/railways\\_and\\_biofuels\\_final\\_report.pdf](https://uic.org/IMG/pdf/railways_and_biofuels_final_report.pdf)
3. Donald A. Heck, Atta Mohammad, and Hind Abi-Akar. A 2,000,000 Mile Evaluation of the Performance and Operational Impacts of B20 Biodiesel Usage in a Long-Haul Trucking Company. Iowa Central Community College, Fort dodge, Iowa, 50501 (D.A.H); and Caterpillar Inc., Mossville, IL, 61552 (A.M., H.A-A.)
4. Hoon Ge, et. al. A Biodiesel Blend Handling Guide. A publication of the: Minnesota Biodiesel Technical Cold Weather Issues Team Handling Subcommittee. Minnesota Departement of Agriculture.
5. L N Komariah et al. Biodiesel effects on fuel filter; assessment of clogging characteristics. 2018 J. Phys.: Conf. Ser. 1095 012017
6. Brandon M. Graver, H. Christopher Frey, and Jiangchuan Hu. Effect of Biodiesel Fuels on Real-World Emissions of Passenger. Locomotives. Environ. Sci. Technol. DOI: 10.1021/acs.est.6b03567

7. Csontos, B., Bernemyr, H., Erlandsson, A.C., Forsberg, O. et al., "Characterization of Deposits Collected from Plugged Fuel Filters," SAE Technical Paper 2019-24-0140, 2019, doi:10.4271/2019-24-0140.
8. Csontos, B., Alim, R., Bernemyr, H., Hittig, H. et al., "Contaminants Affecting the Formation of Soft Particles in Bio-Based Diesel Fuels during Degradation," SAE Technical Paper 2019-01-0016, 2019, doi:10.4271/2019-01-0016.
9. Jim Barker, Paul Richards, Mark Goodwin, Jonathan Wooler. Influence of High Injection Pressure on Diesel Fuel Stability: A Study of Resultant Deposits. SAE Paper number 2009-01-1877 © 2009 SAE International.
10. Mathieu Petiteaux and Guy Monsallier. Impacts of Biodiesel Blends on Fuel Filters Functions Laboratory and Field Tests Results. Copyright © 2009 SAE International.
11. Richard Nelson, Ph.D. Current Status of Biodiesel in Railroads and Technical Issues. November 2012. Moving Forward. Final Report To: National Biodiesel Board.
12. M. Lammert, R. Barnitt, and R.L. McCormick. Field Evaluation of Biodiesel (B20) Use by Transit Buses. Copyright © 2009 SAE International
13. M. Maruf and I. Haryono, "An Effect Of Biodiesel (B20) On Life Time Locomotive Fuel Filter," Maj. Ilm. Pengkaj. Ind., vol. 13, no. 3, pp. 201–208, 2020, doi: 10.29122/mipi.v13i3.3787.
14. Groenewoud, W. M. (2001) 'Thermogravimetry, Chap. 2', Characterisation of Polymers by Thermal Analysis, pp. 61–76.
15. Dir. Jend. EBTKE, 2018, Laporan Kajian dan Uji Jalan (Rail Test) Penggunaan Biodiesel 20% (B20) Pada PT Kereta Api Indonesia (Persero), Direktorat Jenderal Energi Baru, Terbarukan Dan Konservasi Energi Kementerian Energi Dan Sumber Daya Mineral

## Tables

Due to technical limitations, table 1 to 7 is only available as a download in the Supplemental Files section.

## Figures

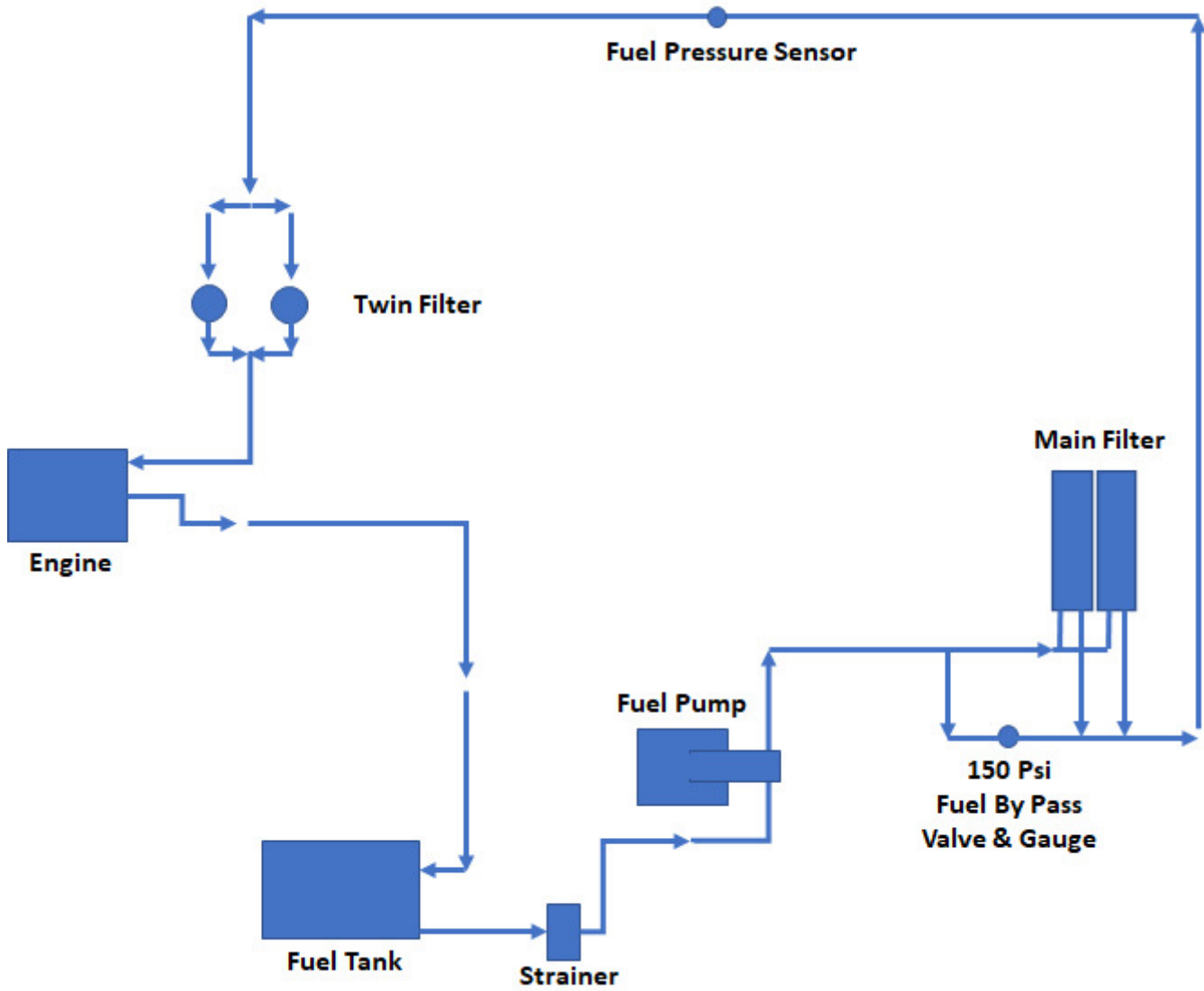


Figure 1

The fuel filtration system of the test locomotive engine

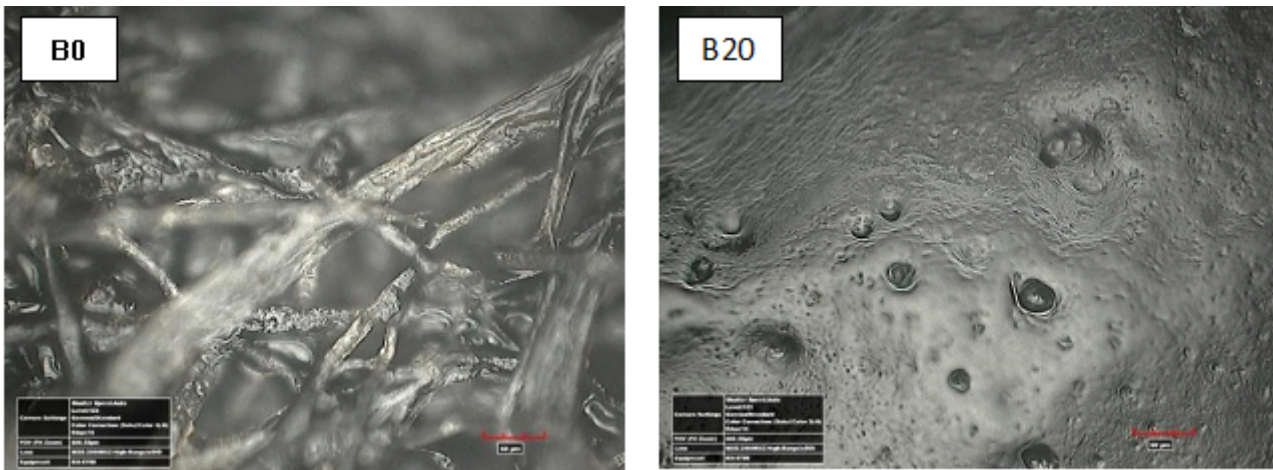
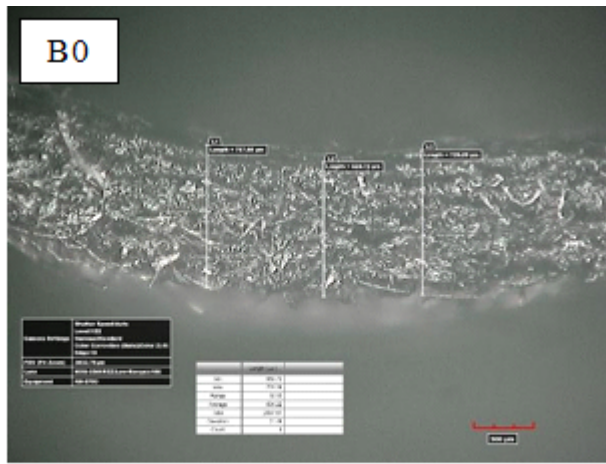
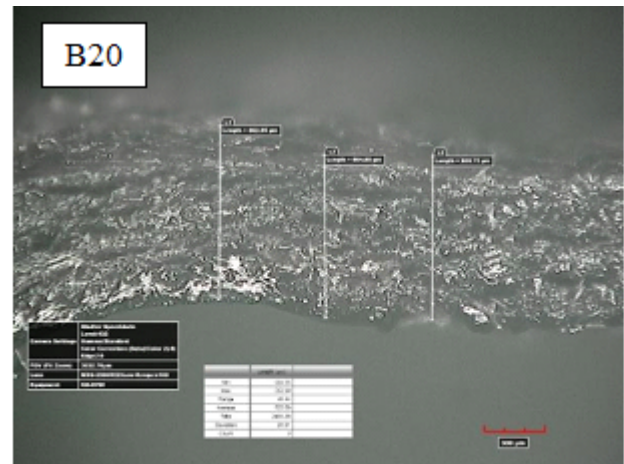


Figure 2

The surface morphology of the locomotive main filter sample after 3 months of use



Thickness average 699  $\mu\text{m}$



Thickness average 822  $\mu\text{m}$

Figure 3

The thickness of the deposit on the locomotive's main filter after 3 months of use

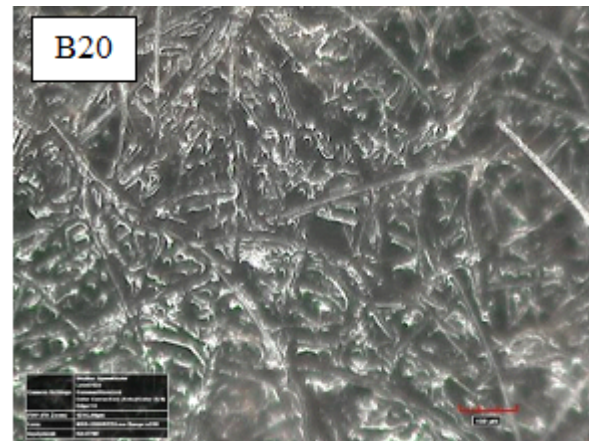
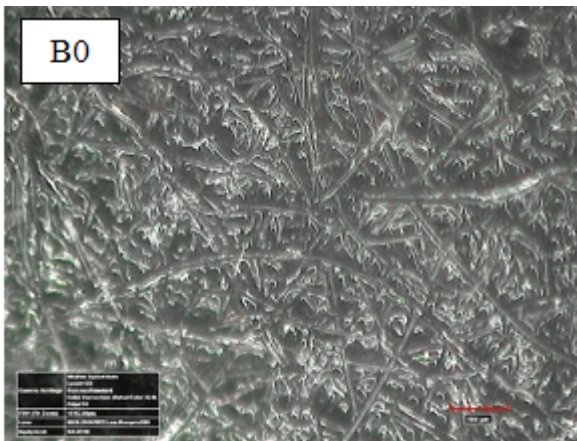
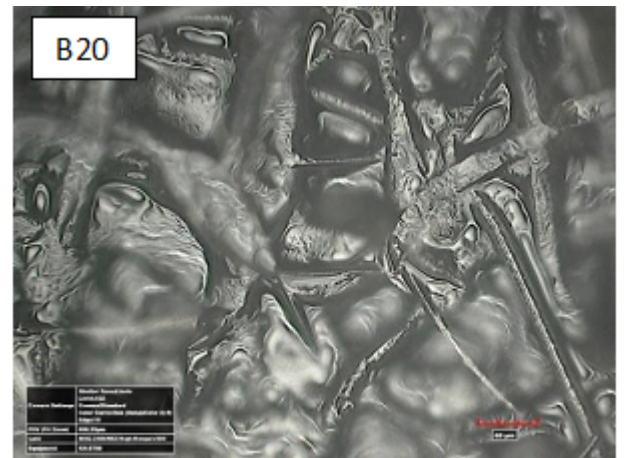
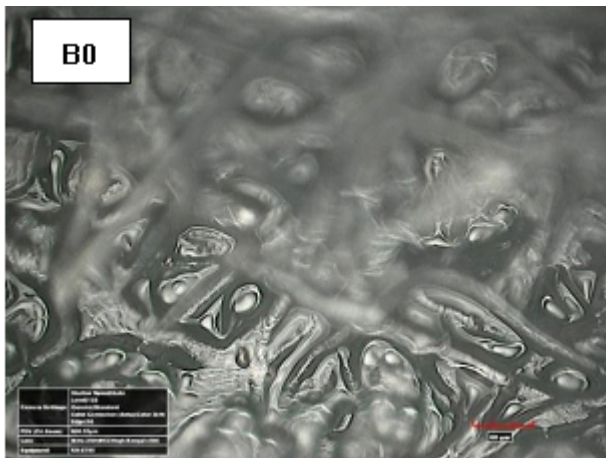


Figure 4

Photo of the used twin filter sample surface after 3 months of use

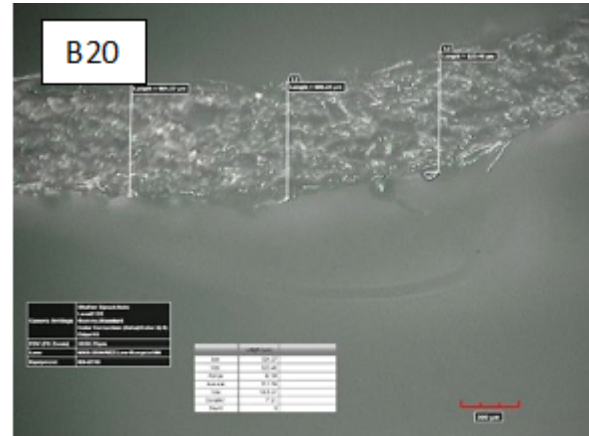


**Figure 5**

Photo of the used twin filter sample surface after 3 months of use



Thickness Average 621  $\mu\text{m}$



Thickness Average 601  $\mu\text{m}$

**Figure 6**

Side view of the used twin filter sample after 3 months of use

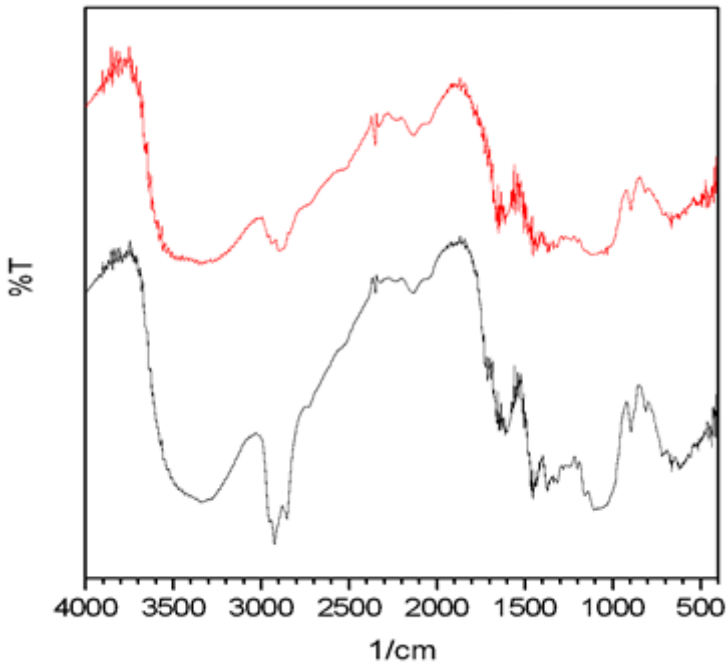
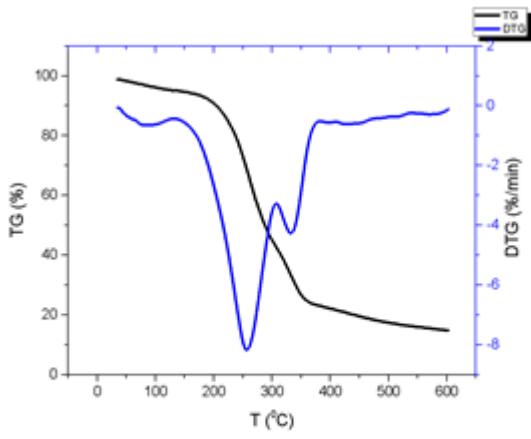
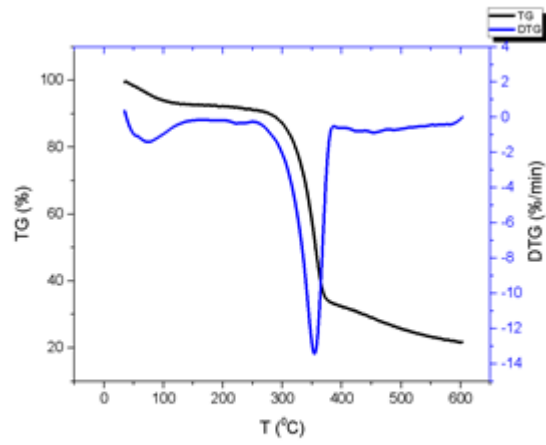


**Figure 7**

Overlay of FTIR analysis results from a used filter with B20 fuel (black graph) and a new filter (red graph)



(a)



(b)

**Figure 8**

TG and DTG graphs for the used filter (a) and new filter (b)

## Supplementary Files

This is a list of supplementary files associated with this preprint. Click to download.

- [Tables.docx](#)